Biomedicine & Pharmacotherapy 168 (2023) 115772

Contents lists available at ScienceDirect

Biomedicine & Pharmacotherapy

journal homepage: www.elsevier.com/locate/biopha

Sarsasapogenin inhibits YAP1-dependent chondrocyte ferroptosis to alleviate osteoarthritis

Ruihan Chen, Chenting Ying, Yuxuan Zou, Changjian Lin, Qiangchang Fu, Zhihui Xiang, Jiapeng Bao *, Weiping Chen *

Department of Orthopedics Surgery, The Second Affiliated Hospital of Medical College, Zhejiang University, Jie Fang Road 88, 310009 Hangzhou, China

ARTICLE INFO

Keywords:
Osteoarthritis
Pharmacology
Ferroptosis
Cell signaling
Hippo signaling pathway

ABSTRACT

The involvement of chondrocyte ferroptosis in the development of osteoarthritis (OA) has been observed, and Sarsasapogenin (Sar) has therapeutic promise in a variety of inflammatory diseases. This study investigates the potential influence of Sar on the mechanism of chondrocyte ferroptotic cell death in the progression of osteoarthritic cartilage degradation. An in vivo medial meniscus destabilization (DMM)-induced OA animal model as well as an in vitro examination of chondrocytes in an OA microenvironment induced by interleukin-1β (IL-1β) exposure were employed. Histology, immunofluorescence, quantitative RT-PCR, Western blot, cell viability, and Micro-CT analysis were utilized in conjunction with gene overexpression and knockdown to evaluate the chondroprotective effects of Sar in OA progression and the role of Yes-associated protein 1 (YAP1) in Sar-induced ferroptosis resistance of chondrocytes. In this study we found Sar reduced chondrocyte ferroptosis and OA progression. And Sar-induced chondrocyte ferroptosis resistance was mediated by YAP1. Furthermore, infection of siRNA specific to YAP1 in chondrocytes reduced Sar's chondroprotective and ferroptosis-suppressing effects during OA development. The findings suggest that Sar mitigates the progression of osteoarthritis by decreasing the sensitivity of chondrocytes to ferroptosis through the promotion of YAP1, indicating that Sar has the potential to serve as a therapeutic approach for diseases associated with ferroptosis.

1. Introduction

OA is a prevalent joint disease globally, predominantly responsible for chronic pain and functional limitations among the elderly population [1,2]. OA can be attributed to a multitude of factors, such as advanced age, physical injury, excessive body weight, psychological tension, and inherent joint irregularities [3,4]. The main characteristic of OA is the deterioration of joint tissue resulting from an imbalance between cartilage and other joint tissues' anabolic and catabolic processes [5,6]. The process of degradation is accompanied by a range of pathological alterations, including subchondral bone sclerosis, synovitis, and inflammatory changes of the tendon and joint capsule [7,8]. The evolution of OA is directly correlated with the catabolic matrix-degrading enzymes' destruction of cartilage extracellular matrix (ECM) [9,10]. Articular cartilage is a connective tissue composed solely of chondrocytes, which are in charge of generating ECM [11,12]. Research suggests that osteoarthritis degradation and articular cartilage homeostasis hinge on chondrocyte survival and anabolic/catabolic balance [13]. The significance of chondrocyte damage is widely recognized in relation to the processes of cell necrosis, apoptosis, and autophagic cell death [14]. Recent researches have found the phenomenon of ferroptosis represents a unique and well-defined mechanism of controlled cellular demise, initially elucidated by Dixon et al. in 2012 [15]. This cellular death exhibits distinct morphological, biochemical, genetic, and immunological attributes that set it apart from alternative modes of controlled cellular death.

Ferroptosis, a type of oxidative cell death, which is characterized by the fatal accumulation of lipid hydroperoxides in an iron-dependent manner [15–17]. Based on recent investigations, it has been determined that glutathione peroxidase 4 (Gpx4) serves as the principal modulator of ferroptosis [18]. Gpx4 employs reduced glutathione (GSH) as a substrate to catalyze the conversion of phospholipid hydroperoxides into lipid alcohols, thereby acting as a protective mechanism against the occurrence of ferroptosis [19,20]. And the system Xc- specific subunit Slc7a11, a typical ferroptosis marker, when inhibited, results in the depletion of intracellular GSH, iron-dependent lipid peroxidation, and

* Corresponding authors.
E-mail addresses: baojiapeng1@zju.edu.cn (J. Bao), ze_cwp@zju.edu.cn (W. Chen).

https://doi.org/10.1016/j.biopha.2023.115772
Received 23 August 2023; Received in revised form 14 October 2023; Accepted 20 October 2023
Available online 24 October 2023

subsequently ferroptosis [21]. Acsl4 (Acyl-CoA synthetase long-chain family member 4), serves as both a biomarker and an inducer to the process of ferroptosis. Lipid hydroperoxides produced by the iron-containing enzyme lipoxygenase, which functions by activating Acsl4-dependent lipid biosynthesis [22]. Various degenerative conditions, including Alzheimer's disease, Parkinson's disease, kidney diseases, cancer, intracerebral hemorrhage, ischemia-reperfusion damage, and stroke, have shown encouraging results in the context of ferroptosis therapy [23]. Recent research has yielded empirical support for the existence of ferroptosis in OA and have identified Gpx4 as a significant regulator of OA [24]. Additionally, chondrocytes that imitate the OA phenotype demonstrated a preference for internalizing iron [25,26].

Sarsasapogenin (Sar), a steroidal sapogenin, which is derived from the rhizome of Anemarrhena asphodeloides Bunge, a plant classified as a Chinese Materia Medica. Extensive research has demonstrated the potential therapeutic effects of Sar in various human disease conditions. For instance, Sar has been proved to have positive effects on Alzheimer-like encephalopathy in diabetes [27]. Lim SM, et al. found that Sar ameliorates colitis in mice by supressing NF-κB and MAPK activation [28], which contributes to the advancement of OA [29]. The roles of Sar in neuro metabolism, apoptotic effect, anti-inflammatory activity, and immune responses are supported by empirical evidence [27,28,30,31,32]. The correlation between Sar and chondrocyte ferroptosis needs to be clarified in order to focus on the function of chondrocyte ferroptosis in OA.

Yes-associated protein 1 (YAP1), a crucial effector in the Hippo signaling pathway, is recognized for its role in controlling the dimensions of various organs and facilitating tissue regeneration [33,34]. In OA progression, the role of YAP in osteoarthritis has been demonstrated to be indispensable and sufficient in maintaining the equilibrium of cartilage, by performing as a key catabolic transcription factor. YAP is both required and sufficient to impede the course of OA by suppressing inflammatory responses triggered by NF-κB signaling [35,36]. Recent research has also demonstrated the indispensability of YAP for modulating cellular iron homeostasis and ferroptosis susceptibility in the context of tumor research, which indicates the potential association between YAP pathway and ferroptosis [37,38]. But it has not yet been determined whether YAP contributes to chondrocyte ferroptosis, how it is regulated in OA, or how it is controlled.

This study employs Interleukin-1 Beta (IL-1β) to induce inflammation, and erastin to induce iron overload in vitro. Furthermore, we generated an OA model in rats through the implementation of surgery-induced DMM. Our study's results validate the involvement of ferroptosis in the pathogenesis of OA and demonstrate the chondroprotective effects of Sar in inhibiting YAP1-dependent chondrocyte ferroptosis, thereby impeding OA progression. We recommend that the inhibition of ferroptosis could be a promising alternative approach for the treatment of osteoarthritis.

2. Materials and methods

2.1. Reagent

The following reagents were acquired from Gibco BRL: foetal bovine serum (FBS), penicillin/streptomycin, Dulbecco's modified Eagle's medium (DMEM), and 0.25 % trypsin. The collagenase II enzyme was acquired from Sigma—Aldrich, while the recombinant rat interleukin-1β (IL-1β) was obtained from R&D Systems. Plasmid (pEX-3(pGCMV/MCS/Neo) and siRNAs specific to Yap1 were designed with the coding sequences of mouse Yap1 (sense (5′−3′): CUGCCACCAAGUUAGAUAATT; antisense (5′−3′): UUAUCUAACUUGGUGGCAGTT) and GP-transfect-mate were purchased from GenePharma(Shanghai, China).

2.2. Cell isolation, culture and treatment

The approval was granted by the Institutional Animal Care and Use Committee of Zhejiang University, Hangzhou, China. Small pieces of knee articular cartilage were obtained from Sprague—Dawley (SD) rats that were three weeks old. Subsequently, fragments of cartilage were collected and subjected to a subsequent incubation period of 3.5 h, during which they were exposed to a digestion buffer (consisting of DMEM/F12 supplemented with 0.2 % collagenase II) at a temperature of 37 °C. Following filtration and centrifugation at 1000 revolutions per minute for 5 min, the chondrocytes were subsequently introduced into 25 cm2 flasks containing DMEM/F12 medium supplemented with 10 % fetal bovine serum and 1 % penicillin/streptomycin. The chondrocytes in question were classified as passage-0 (P0) chondrocytes. Upon reaching a confluence of approximately 90 %, the chondrocytes underwent passaging at a ratio of 1:3. Subsequently, cells from passages 1–3 (P1–3) were utilized in our study.

The infection procedure involved incubating chondrocytes with siRNA or plasmid (pEX-3) and GP-transfect-mate in a growth medium. After 12 h, the infection medium was replaced with growth medium. Subsequently, chondrocytes exhibiting Yap-1 knockdown and overexpression were employed for subsequent experimental procedures, with a duration of 1 day. The blank control (NC) group consisted of chondrocytes that were transfected with knockdown control siRNA for a duration of 1 day. In order to investigate the impact of Yap-1 in an in vitro inflammatory setting, we employed Yap-1-knockdown (KD) or Yap-1 overexpressing (OE) chondrocytes. These chondrocytes were subjected to IL-1β stimulation for a duration of 24 h following transfection for one day.

2.3. CCK-8 cell viability assay

The CCK-8 assay (KGA317, KeyGen Biotech, Nanjing, China) was employed according to the manufacturer's instructions to examine the impact of Sar on the viability of chondrocytes. The chondrocytes from the second passage were cultured in 96-well plates, with a density of 1.5* 104 cells per well, for a duration of 24 h. Then the cells were cultured in DMEM/F12 medium supplemented with different concentrations of Sar (0, 0.25, 0.5, 1, 1.5, 2, 4, and 8 M) for a duration of either 24 or 48 h, followed by exposure to 10 ng/ml IL-1β. Subsequently, the medium was substituted with DMEM/F12 supplemented with 10 % CCK-8 reagent, and the chondrocytes were incubated for an additional duration of 3 h at a temperature of 37 °C. Following that, the optical density (OD) was assessed at a wavelength of 450 nm utilizing an ultraviolet spectrophotometer.

2.4. RNA isolation and reverse transcription-qPCR

The isolation of total RNA from chondrocytes was performed using Trizol reagent (Invitrogen, CA, USA), followed by reverse transcription to synthesize complementary DNA (cDNA) using the PrimeScriptTM RT Master Mix Kit (Takara Biotechnology Co., Ltd). Subsequently, the quantification of the synthesized cDNA was carried out. The real-time polymerase chain reaction (PCR) was conducted using an Applied Biosystems StepOnePlusTM instrument (Applied Biosystems, United States) and SYBR® Premix Ex TaqTM II reagent (Takara Biotechnology Co., Ltd) in accordance with the manufacturer's instructions. Before amplification, individual samples of 10 μl were prepared. These samples consisted of 5 μl of SYBR® Green, 1 μl of cDNA, 0.8 μl of each primer, and 3.2 μl of

Table 1
Primers for qRT-PCR.

Gene	Forward	Reverse
18S	CCTGAGAAACGGCTACCACA	ACCAGACTTGCCCTCCAATG
MMP3	ACATGGAGACTTTGTCCCTTTTG	TTGGCTGAGTGGTAGAGTCCC
iNOS	AGTCAACTACAAGCCCCACG	AGAAACTTCCAGGGGCAAGC
MMP9	GATCCCCAGAGCGTTACTCG	GTTGTGGAAACTCACACGCC
MMP13	CTGGGCCCTGAATGGGTATG	CTCAAAGTGAACCGCAGCAC

ddH2O. The primer sequences derived from established GenBank sequences are provided in Table 1. The 18 s gene was employed as the internal reference gene. All of the aforementioned experiments were conducted in triplicate in accordance with the instructions provided by the manufacturer. The mRNA expression data of the aforementioned genes were subjected to analysis utilizing the $2 - \Delta\Delta Ct$ formula.

2.5. MDA, GSH and SOD assay

The concentration of malonaldehyde (MDA), content of GSH, and total activity of superoxide dismutase (SOD) were assessed in P1–3 chondrocytes using the protocols provided by the manufacturer. To facilitate the process of detection, the utilization of the following kits has been employed: the Lipid Peroxidation MDA Assay Kit (Beyotime, S0131), the GSH and GSSG Assay Kit (Beyotime, S0053), and the Total Superoxide Dismutase Assay Kit with WST-8 (Beyotime, S0101).

2.6. Detection of intracellular ROS

The measurement of intracellular levels of reactive oxygen species (ROS) was conducted using DCFH-DA fluorescent probes, following the instructions provided by the manufacturer. In summary, prior to treatment, chondrocytes underwent a triple wash with phosphate-buffered saline (PBS). Subsequently, they were subjected to a 20-minute treatment with 10 M DCFH-DA at a temperature of 37 ∘C, while being kept in darkness. Following the designated incubation period, the cells underwent a rinsing process utilizing phosphate-buffered saline (PBS) and were subsequently subjected to examination using an inverted Lecia Fluorescence Microscope.

2.7. Immunofluorescence

The cells that were subjected to treatment were placed in 6-well plates. These cells were then permeabilized for a duration of 5 min using a solution containing 0.1 % v/v Triton X-100. Following permeabilization, the cells were blocked for a period of 1 h using a solution containing 5 % BSA. Subsequently, the cells were incubated with a primary antibody overnight at a temperature of 4 ∘C. Following three washes in phosphate-buffered saline (PBS), the cells underwent a two-hour incubation period in the absence of light with appropriate fluorescent secondary antibodies and 4′,6-diamidino-2-phenylindole (DAPI). The cells were examined utilizing a fluorescence microscope.

2.8. Western Blot

Following the treatment, the chondrocytes underwent a triple wash with phosphate-buffered saline (PBS) prior to their isolation using a cell scraper. Following that, the cells that were acquired were subjected to lysis using RIPA Lysis Buffer (P0013B, Beyotime, China), supplemented with a protease inhibitor cocktail (P1005, Beyotime, China) and a protein phosphatase inhibitor (P1260, Solarbio Science & Technology, Beijing, China). The resulting mixture was then cooled on ice for a duration of 30 min. Following the extraction process, equivalent quantities of protein from each sample were subjected to separation via SDS-PAGE, employing a 10 % gel, and subsequently transferred onto polyvinylidene difluoride membranes using electrotransfer. The company identified as IPVH00010, operating under the name Millipore, is located in the United States. Subsequently, the membranes were subjected to blocking using a 10 % milk solution in TBST for a duration of 2 h at ambient temperature. Then the membranes were subjected to treatment with the primary antibody at a temperature of 4 °C for a duration of overnight. The membrane underwent incubation with secondary antibodies (A0208, A0216; 1: 5000, Beyotime, China) specific to goat anti-rabbit and anti-mouse for a duration of 2 h at room temperature on the subsequent day, after being subjected to three washes with TBST. The ECL kit was used to determine the luminescence (WBKLS005, Immobilon, KGaA). GAPDH (GA) was employed as an endogenous control and ImageJ was used to examine the relative amounts of proteins. Triplicates of each assay were run.

2.9. Animal experiments

The experiments conducted on animals were approved by the Ethics Committee of The Second Affiliated Hospital, School of Medicine, Zhejiang University, Hangzhou, China. For our in vivo investigation, we employed 15 male Sprague-Dawley (SD) rats, 6 weeks old, separated into 3 groups: Sham, DMM, Sar-treated ($n = 5$ in each group). Rats were bred in a clean, pathogen-free vivarium with a regular 12-hour day/night cycle, eating standard rat food, and drinking water.

In order to induce osteoarthritis, DMM surgery was conducted on rats. To administer anesthesia, pentobarbital was injected into the peritoneal cavity of the rats. Subsequently, the knee joints were exposed and incised medially through a parapatellar approach. In both the DMM and DMM+Sar groups, the transection of the medial meniscotibial ligament (MMTL) occurred without any concurrent injuries to the ligament or cartilage. In contrast, within the control group, a comparable surgical incision was executed without the transection of the medial meniscotibial ligament (MMTL). After one week, rats in the Sar-treated received injections of precise dosation of Sar into the knee articular cavity. We calculated the dosation of the Sar by 10 mg per kg of the weight, the concentration of Sar is 5 μM. The rats in the Sham and DMM groups were given physiological saline injections once a week. The rats were euthanized after 12 weeks, and the knee joints were fixed in 4 % paraformaldehyde solution, and the specimens were decalcified for 3 weeks with 10 % EDTA before being embedded in paraffin.

2.10. Histological analysis

During a duration of two months, the fixed knee joints underwent decalcification using a 10 % EDTA solution. The specimens underwent dehydration using a series of ascending ethanol concentrations, followed by embedding in paraffin blocks and subsequent sectioning into 5 μm slices. The joint sections were subsequently stained with Sudan III (SO) and Hematoxylin and Eosin (HE) as per the guidelines provided by the manufacturer. Subsequently, sections were subjected to immunohistochemistry analysis.

2.11. Micro-CT analysis

In summary, the joint specimens were immobilized in a 4 % paraformaldehyde (PFA) solution and subsequently preserved in a 70 % ethanol solution. The high-resolution micro-CT (80490, MILabs BV, Netherlands) was utilized to capture images of rat knee joints, with an isometric resolution of 20 m. Subsequently, the acquired images were subjected to analysis via three-dimensional model visualization software (IMALYTICS Preclinical, version 2.1). Additionally, microtomographic data were employed to evaluate quantitative morphometry indices pertaining to the subchondral bone, including trabecular thickness (Tb.Th), bone volume fraction (BV/TV), and trabecular separation (Tb.Sp).

2.12. Statistical analysis

The outcomes are presented as the mean ± standard error ($n \geq 3$) of the mean of independent replicates. Statistical significance was evaluated by employing the two-tailed Student's t-test or one-way analysis of variance (ANOVA) to compare the two groups. Subsequently, the Tukey's test was utilized for conducting multiple comparisons. The p values were represented in accordance with the New England Journal of Medicine (NEJM) format, where "NS" denoted no significant difference, "* " denoted $p < 0.05$, "**" denoted $p < 0.01$, and "*** " denoted $p < 0.001$. The statistical analyses were conducted using GraphPad Prism 9.

3. Results

3.1. The effect of Sar on chondrocyte viability

Fig. 1A depicts Sar's structural formula. The cell counting kit (CCK-8) assay was used to initially determine Sar's cytotoxicity on chondrocyte viability. As illustrated in Fig. 1B–C, the concentration of ≤ 16 μM was observed. At both 24 and 48 h, it was observed that Sar did not exhibit obvious toxicity towards rat chondrocytes under the concentration of 4 μM. Hence, the concentrations of 1, 2, and 4 μM were chosen for subsequent in vitro experiments.

3.2. Sarsasapogenin inhibits matrix-degrading genes and inflammation-induced degradation of cartilage

We next investigated the effect of Sar in vitro chondrocyte catabolism caused by IL-1β, in order to better understand the role of Sar in the progression of OA. We used IL-1β, which is a joint inflammation factor, to induce chondrocytic inflammation. The results obtained from the cell counting kit (CCK-8) assay indicated that chondrocytes exhibited no signs of toxicity when exposed to moderate concentrations of Sar over a 48-hour period. The RT-qPCR results showed that catabolic gene mRNA levels (MMP3, MMMP9, MMP13, and iNOS) were significantly reduced in IL-1β-treated chondrocytes (Fig. 2A). Additionally, the Western blot analysis demonstrated that the heightened protein expression levels of MMPs, Cox2, and iNOS in the Sar groups were effectively attenuated in a manner that was dependent on the dosage (Fig. 2B and C). In the interim, Sar effectively suppressed the IL-1β-induced decrease in extracellular matrix constituents (collagen II and aggrecan) as well as Sox9 expression (Fig. 2B and C). Consequently, the findings showed that Sar exhibits a protective effect on rat chondrocytes through the inhibition of inflammatory and matrix-degrading gene expression, coupled with an upregulation of cartilage-specific gene expression.

3.3. Sar alleviates OA progression and cartilage degeneration in a rat DMM model

In order to investigate the role of Sar in OA progression, we compared cartilage degeneration and gene expression following DMM surgery with (DMM + Sar group) or without (DMM group) Sar application (Fig. 3A). Safranin O and H&E (Hematoxylin-eosin) staining of cartilage, as well as Osteoarthritis Research Society International (OARSI) score analysis [39], revealed that cartilage degeneration occurred after DMM surgery. In the DMM + Sar group as compared to the DMM group, articular cartilage degradation was reduced along with a considerably lower OARSI grading score (Fig. 3B, C).

To validate the preventive effects of Sar in the context of OA induced by DMM, we employed immunohistochemistry as a means to examine the expression patterns of specific proteins associated with OA in tissue samples. In comparison to the DMM group, the findings indicated a notable increase in collagen II expression in the Sar-treated groups, accompanied by a significant decrease in MMP13 expression (Fig. 3D-E).

We next utilized micro-CT imaging to assess the radiological alterations in rat joints. The whole joint 3D reconstruction results revealed that DMM rats developed marginal osteophytes and other alterations around the articular surface, whereas Sar treatment reduced the osteophytes and alterations, proving that Sar treatment could significantly impede the progression of OA (Fig. 3F; The OA alterations were marked by red arrow). The development of bone cysts is a discernible characteristic of advanced osteoarthritis, as evidenced by a 3D reconstruction

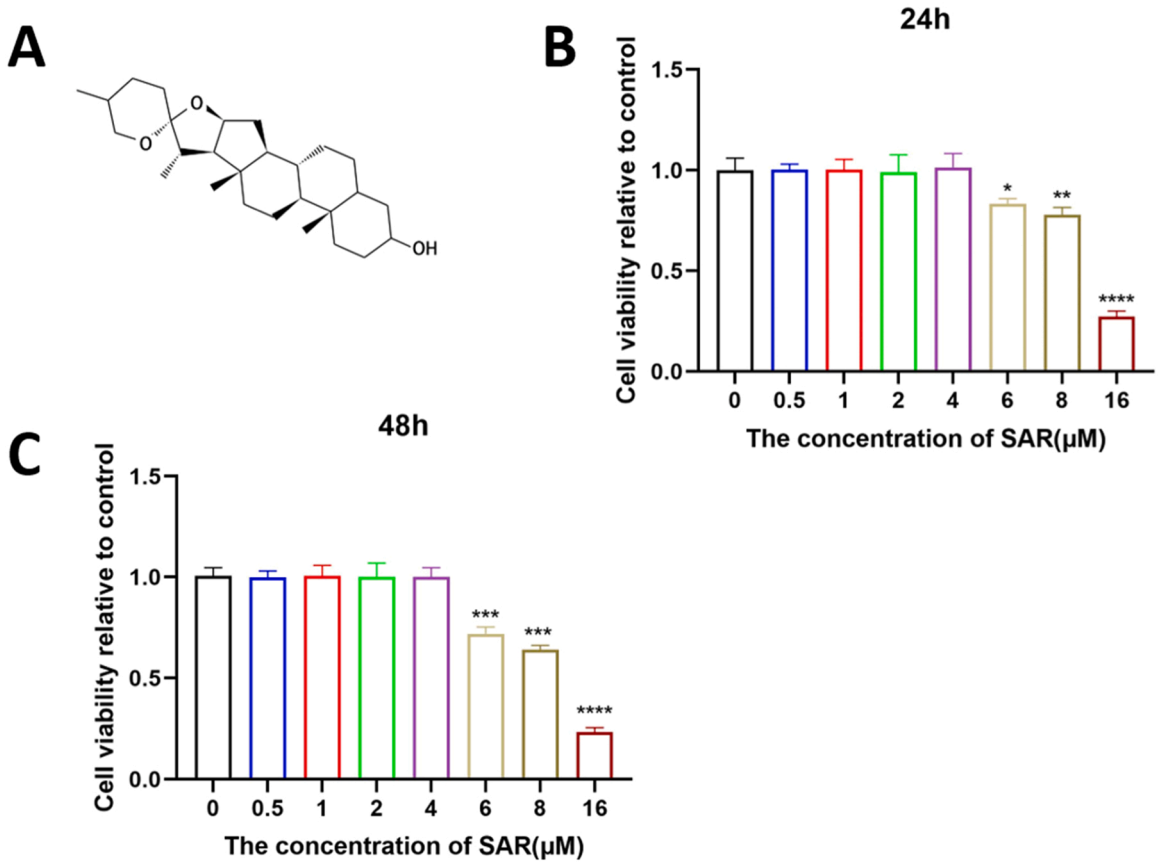

Fig. 1. Effects of Sar on chondrocyte viability. A) Structural formula of Sar. B - C) Cells were treated with the indicated concentrations of Sar for 24 and 48 h. Rat chondrocyte viability was evaluated by CCK-8 assay. All experiments were repeated independently three times. Values are expressed as mean ± SD; *$p < 0.05$, **$p < 0.01$, ***$p < 0.001$, and ****$p < 0.0001$ vs. the control group.

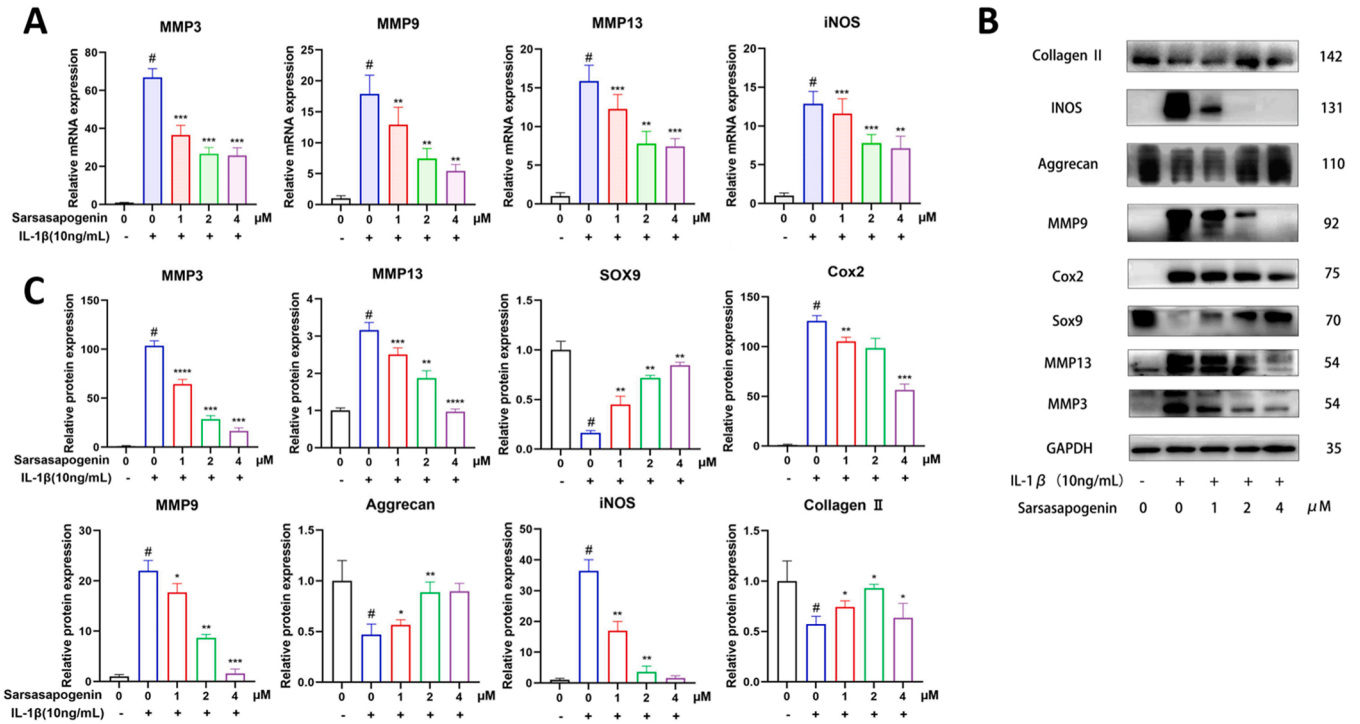

Fig. 2. Sar reduced matrix-degrading gene expression and inflammation-induced cartilage degradation. A) Gene expression analysis of MMP3, MMP9, MMP13, and iNOS in rat chondrocytes treated with IL-1β. B-C) Representative Western blots and quantification data of collagen II, iNOS, aggrecan, Cox2, Sox9, MMP3, MMP9, and MMP13 in rat chondrocytes after treatment with IL-1β, respectively. Values are expressed as mean ± SD, n = 3; #p < 0.05 vs. control group, *p < 0.05, **p < 0.01, ***p < 0.001, and ****p < 0.0001 vs. model group.

of the subchondral bone structures in the tibia. The presence of bone cysts was readily apparent in the group of DMM models, and the treatment with Sar effectively reversed this observation (Fig. 3F). In addition, three trabecular bone indices were calculated in this study: trabecular bone volume fraction (BV/TV), trabecular thickness (Tb.Th; cm), and trabecular spacing (Tb.Sp; cm). The findings showed that DMM surgery significantly reduced BV/TV and Tb.Th, while increasing Tb.Sp. Sar treatment significantly reduced the alterations (Fig. 3G), proving that Sar therapy could prevent the progression of OA while maintaining the microarchitecture of the tibial subchondral bone. When taken as a whole, these findings show that Sar can prevent DMM-induced osteoarthritis in vivo.

3.4. Sar protects osteoarthritic chondrocytes by reducing ferroptosis sensitivity

According to recent research, there exists a connection between chondrocyte ferroptosis and the maintenance of chondrocyte homeostasis, as well as the degeneration of cartilage in individuals with osteoarthritis [24]. Firstly, we observed whether Sar could reduce the ferroptosis in vitro. Western blotting revealed that in chondrocytes, the presence of IL-1β decreased the expression of Gpx4 and Slc7a11 while increasing the protein level of Acsl4. To our surprise, Sar not only reversed the declines of the expression of Gpx4 and Slc7a11 and the increase of Acsl4, but Sar also overexpressed the Gpx4 and Slc7a11 while knocked down the expression of Acsl4 in a dose-dependent manner (Fig. 4A-B). Using an immunofluorescence staining test, we investigated the proportion of Gpx4+ and Acsl4+ chondrocytes in the normal control, IL-1β-treated group, and Sar -treated IL-1β-groups. The proportion of Gpx4+ chondrocytes in the IL-1β treatment group exhibited a significant decrease compared to the control group, and the Sar treatment obviously reversed this decrease. And the Acsl4+ chondrocytes in the IL-1β group increased sharply comparing to the control group, and this change was also suppressed by the treatment of Sar (Fig. 4C-D). SOD activity was also boosted after Sar treatment, indicating a reduced level of oxidative stress (Fig. 4E). We also looked into intracellular ROS levels, which always rise sharply during ferroptosis. As anticipated, subsequent to Sar treatment, a notable decrease in ROS levels was observed in normal chondrocytes compared to those treated with IL-1β, as evidenced by the results of DCFH-DA staining (Fig. 4F). Furthermore, Sar significantly reduced the quantity of MDA, a byproduct of lipid peroxidation (Fig. 4G). The amount of GSH was also investigated as a lowering substrate of Gpx4 action. GSH was depleted in IL-1β treated chondrocytes, and GSH/GSSG levels were also reduced in the IL-1β treated groups, and Sar inhibited the downtrends (Fig. 4H). The association between ferroptosis and lipid droplets (LDs) has recently been established, wherein LDs have been observed to accumulate and enhance the susceptibility of cancer cells to ferroptosis [40–42]. Nile Red was used to stain the LDs, and we discovered that they were significantly less abundant in IL-1β+Sar-treated cells than in IL-1β--treated cells (Fig. 4I).

We next used an immunohistochemical staining test to determine the proportion of Gpx4 +and Slc7a11+ chondrocytes in the Sham-operated, DMM, and Sar-treated DMM groups in order to evaluate the function of Sar in chondrocyte ferroptosis (Fig. 4J). The percentage of Gpx4+ chondrocytes in the DMM group was significantly lower than in the sham group, while the percentage of Acsl4+ chondrocytes was apparently increased in the DMM group, as expected (Fig. 4K). These in vivo findings suggested that Sar treatment could significantly mitigate OA-induced chondrocyte ferroptosis.

Furthermore, transmission electron microscopy (TEM) was used to detect morphological alterations in mitochondria, which are a hallmark of ferroptosis. Based on ultrastructural analysis, the chondrocytes observed in the OA model exhibited characteristic phenotypes. These included a decrease in mitochondrial ridge, condensed mitochondrial membrane densities, a decrease or absence of mitochondria crista, and breakage of the outer mitochondrial membrane (OMM). Notably, the nucleus appeared to be unaffected and maintained its normal structure.

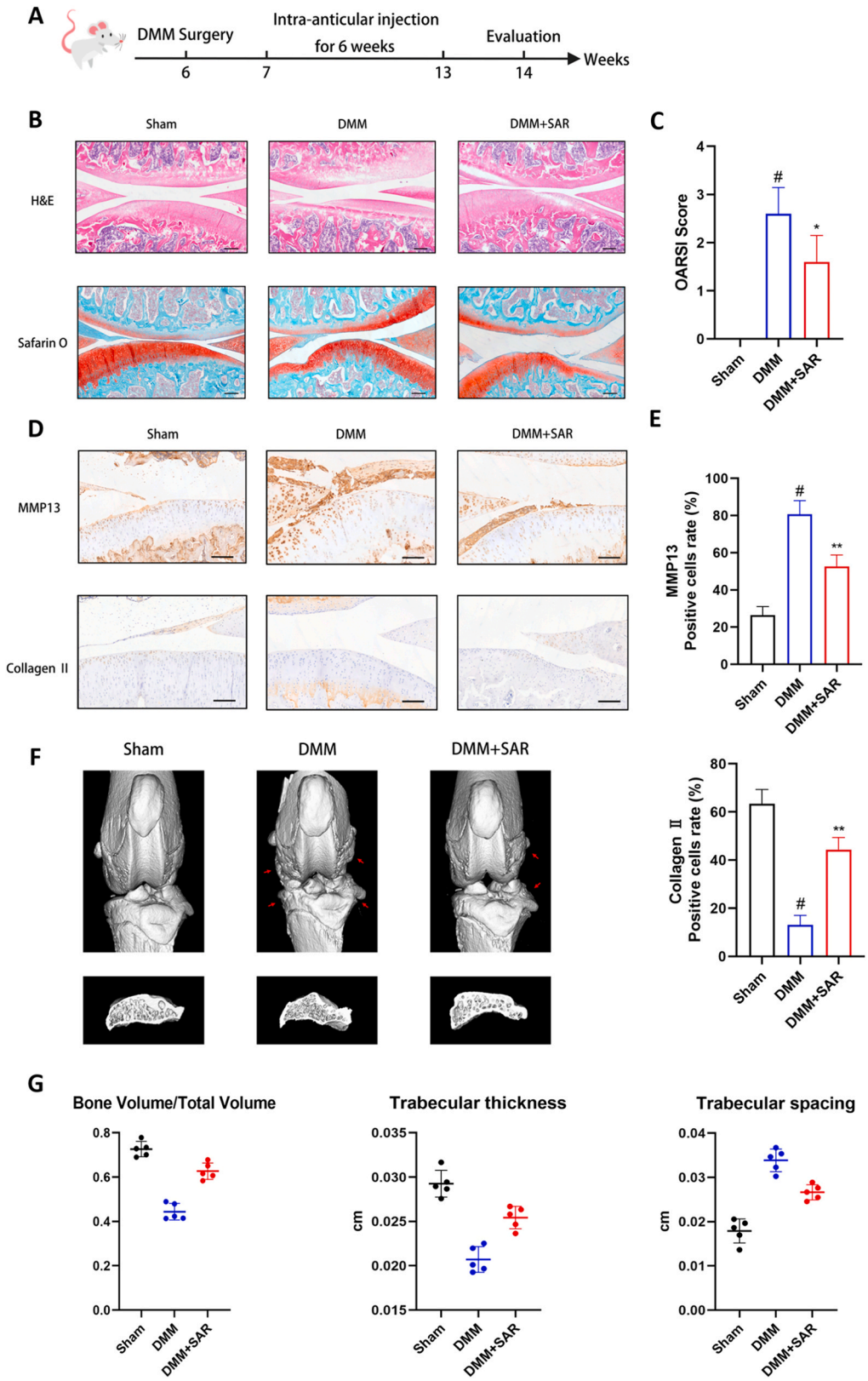

Fig. 3. Sar alleviates OA progression and cartilage degeneration in the rat DMM model. A) The procedure flow chart for animals. B) Images of safranin O staining and HE staining of rat knee joints. Scale bars = 200 μM. C) The OARSI score was used to quantify the severity of OA in rats. D) Immunohistochemistry for antibody against MMP13 and collagen II. Scale bars = 200 μM. E) Quantitative analysis for immunohistochemistry. F) Reconstruction of 3D rat knee models and subchondral bone in each group. G) IMALYTICS Preclinical 2.1 software was used to evaluate BV/TV, Tb.Th, and Tb.Sp. Values are expressed as mean ± SD, n = 5. #$p < 0.05$ vs. sham group, **$p < 0.01$, and ****$p < 0.0001$ vs. DMM group.

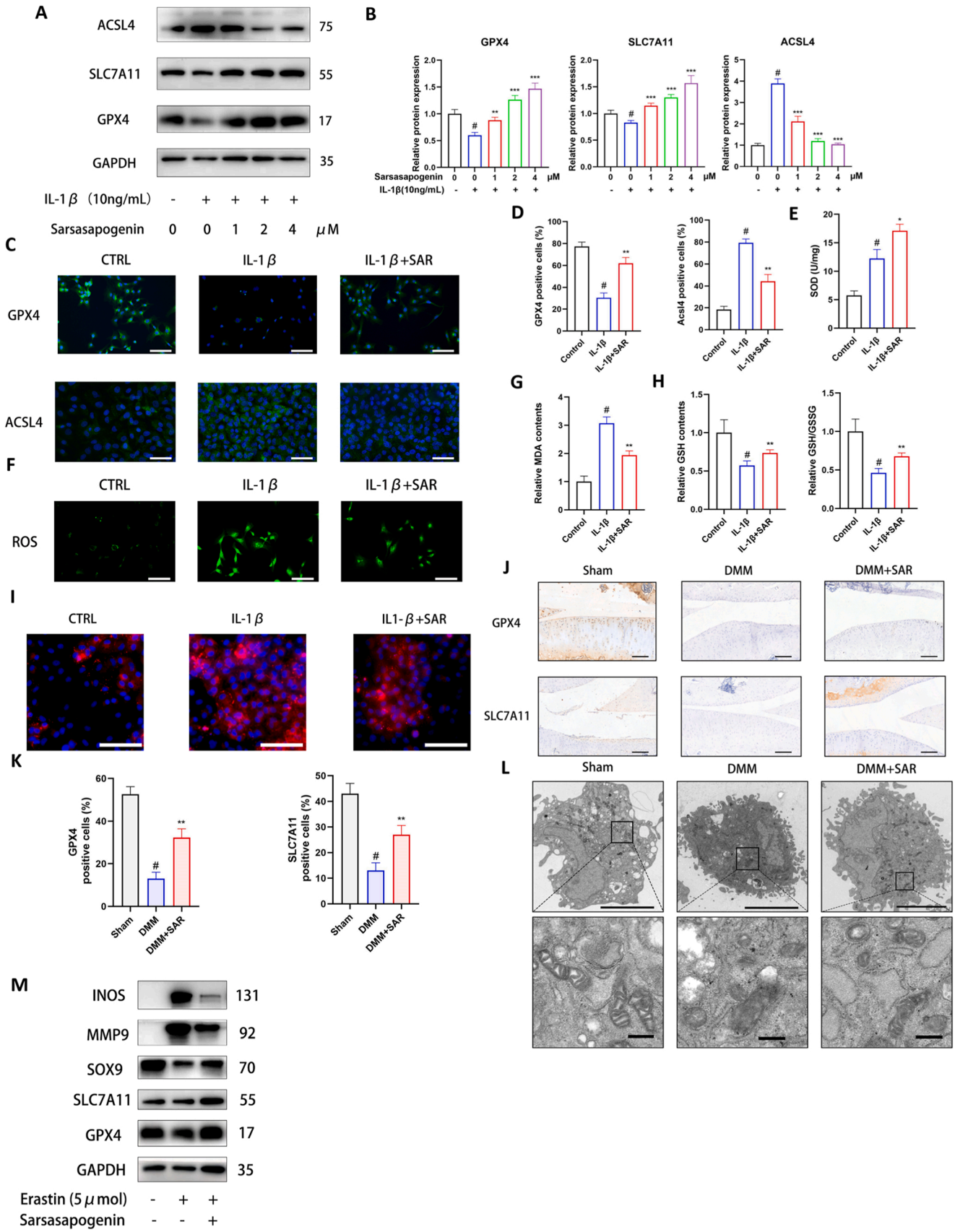

(caption on next page)

Fig. 4. Sar protects chondrocytes in osteoarthritis by reducing their sensitivity to ferroptosis. A-B) Western blotting results and quantitative analysis of the Gpx4, Slc7a11 and Acsl4 of chondrocytes 24 h post indicated treatments. n = 3. C-D) Immunofluorescence for antibody against GPX4 and Acsl4 and quantitative analysis. Green, GPX4 and Acsl4; Blue, DAPI; Scale bar = 100 μm; Chondrocytes pretreated with or without Sar (4 μM) or IL-1β. E) SOD activity in chondrocytes was measured 24 h after the appropriate treatments. n = 3. F) The ROS level of chondrocytes was measured by DCFH-DA 24 h after the prescribed treatments. n = 3. Scale bars= 100 μm. G) MDA measurement 24 h post prescribed treatment. n = 3. H) GSH contents and ratio of GSH/GSSG measurements. n = 3. I) Representative images of chondrocytes 24 h post prescribed treatments stained with Nile Red to detect LDs. Scale bars= 100 μm. J-K) Immunohistochemistry and quantitative analysis for antibody against GPX4 and Slc7a11. Scale bars = 200 μM. L) Transmission electron micrographs of OA cartilage samples demonstrating morphological alterations in mitochondria. Scar bars, up, 5 μM; down, 400 nm. M) Western blotting results of the ferroptosis, anabolic and catabolic gene expression of chondrocytes 24 h post treatments with or without erastin (5 μmol) after treatment of Sar (4 μM). All quantified data are shown as mean ± SD; #$p < 0.05$, *$p < 0.05$, **$p < 0.01$, ***$p < 0.001$ by one-way ANOVA followed by the Tukey- Kramer test.Sorption selectivity.

As is exhibited in the figures, intra-articular injection of Sar could unambiguously avoid ultrastructural and morphological changes to the OA chondrocytes (Fig. 4L).

Erastin is an effective inducer of ferroptosis and a metabolically stable inhibitor of system Xc- [43]. In line with our findings of IL-1β treatment, we have additionally observed that the administration of Sar dramatically reduced chondrocytic ferroptosis and cellular catabolism brought on by applying erastin. Sar inhibited erastin-induced downregulation of ferroptosis components (Gpx4 and Slc7a11), while reversed the augment of MMP9 and iNOS and prevented the reduced SOX9. (Fig. 4M). Taken together, according to our findings, Sar protects chondrocytes from OA by inhibiting ferroptosis in the way of limiting lipid accumulation and intracellular ROS.

3.5. Sar reduces chondrocyte ferroptosis sensitivity by increasing YAP1 expression

YAP1 is a crucial anabolic mediator regulated by Hippo signaling in the pathogenesis of OA [35,36]. Since Sar prevents cartilage degradation and chondrocyte ferroptosis, we investigated how YAP1 expression changed in vivo and in vitro in cartilage degeneration models in response to Sar. In vitro, as the Western blotting results shows, the expression of YAP1 was found to be significantly reduced in the group treated with IL-1β, and the decline of YAP1 expression was reversed by the treatment of Sar dose-dependently (Fig. 5A-B). We also discovered that the expression of YAP1 declined in the erastin-treated chondrocytes, and the administration of Sar reduced this decline caused by erastin (Fig. 5C), this indicates that YAP1 comes into antagonism with the progression of ferroptosis. The immunofluorescence results also showed that the IL-1β reduced the expression of YAP1 and the treatment of Sar regained the high expression of YAP1 (Fig. 5D). We next utilized an immunohistochemical staining test to observe the proportion of YAP1+ chondrocytes in the Sham-operated, DMM, and Sar-treated DMM groups. The findings of the study revealed a significant decrease in the proportion of chondrocytes expressing YAP1 in the DMM group compared to the sham group. However, the application of Sar resulted in a restoration of YAP1-positive chondrocytes to a level that closely resembled that of the sham group (Figs. 5, 5E-F). Collectively, the data presented indicate a strong correlation between YAP1 and the progression of osteoarthritis, specifically in relation to ferroptosis.

Since Sar ameliorates cartilage degeneration and chondrocyte ferroptosis, while promoting the expression of YAP1, we examined the potential involvement of YAP1 in the suppression of chondrocyte ferroptosis mediated by Sar. To investigate how YAP1 affects ferroptosis, we utilized plasmid and small interfering RNA which are specific to YAP1 to overexpress or knockdown YAP1 in chondrocytes via transfection. First, we utilized siRNA transfection in chondrocytes to knock down YAP1 expression and found that YAP1 knockdown significantly aggravated the IL-1β-induced downregulated Gpx4 and Slc7a11 expression while exacerbating the IL-1β-induced upregulation of the expression of Acsl4, and we found that the knockdown of YAP1 eliminated the remittance brought by treatment of Sar on the IL-1β-induced ferroptosis-associated changes (Fig. 5G). Second, we overexpressed YAP1 in chondrocytes via plasmid (pEX-3) transfection, in accordance with the expectation, the overexpression of YAP1 regained the declined expression of Gpx4 and Slc7a11 induced by IL-1β, while compromising the increased expression of Acsl4, furthermore, the overexpression of YAP1 played a synergistic role with Sar in promoting both Gpx4 and Scl7a11 that impede ferroptosis and inhibiting the ferroptosis promotor gene Acsl4 (Fig. 5H). Ferrostatin-1 (Fer-1), a suppressor of ferroptosis, were utilized to accurately investigate the involvement of YAP1 in the mechanism by which Sar impedes chondrocyte ferroptosis. The results of the Western blotting showed that erastin eliminated the effect of Sar on genes associated with ferroptosis (Fig. 5I). In the meantime, Fer-1 treatment increased the protective effect of Sar on anti-ferroptosis gene expressions (Fig. 5J).

The results of the TEM analysis also showed that Sar was not successful in effectively mitigating the mitochondrial damage that IL-1β treatment caused in YAP1-knockdown chondrocytes (Fig. 5K). Due to its incapacity to alter LD deposition, in chondrocytes with a knockdown of YAP1, there was no discernible effect of Sar on lipid degeneration (Fig. 5L). Moreover, Sar failed to reduce the level of MDA that was amplified by IL-1β in siYAP1-treated chondrocytes (Fig. 5M). The deletion of GSH amounts and GSH/GSSG levels were also failed to revert by Sar when siYAP1 was applied (Fig. 5N). In addition, the presence of Fer-1 partially counteracted the effect of YAP1 knockdown on the resistance to Sar-induced ferroptosis (Fig. 5, K-N). Together, these findings strongly showed that Sar inhibits the progression of OA through creating a chondroprotective effect by enticing YAP1-mediated chondrocyte insensitivity to ferroptosis.

4. Discussion

OA is the type of arthritis that affects the most people and is the leading cause of long-term disability in older people. In the current research, we discovered that Sar, a steroidal sapogenin, impeded the progression of OA and provided chondroprotection by reducing the chondrocyte sensitivity to ferroptosis. And YAP1 was crucial to this procedure. Downregulation of YAP1 induced chondrocyte ferroptosis and prevented Sar's chondroprotective effects.

It has been established that Sar can be utilized in a number of human disease states. Current findings on Sar are most based on its beneficial effects on diabetes-associated diseases. As for OA, there have been no report showed that Sar has contribution to OA amelioration. But it has been proved that Sar has positive effects on inflammatory diseases. It has been reported that Sar reduced DN (diabetic nephropathy) in rats by downregulating PAR-1 in the kidney, which inhibited the NLRP3 inflammasome and NF-κB pathway [44]. In our study, Sar was successful in downregulating pro-inflammatory factors by inhibiting chondrocyte catabolism both in vivo and in vitro. When compared to the prior research, Sar demonstrated a more potent ability to alleviate colitis in mice. This was accomplished by inhibiting the activation of pathways known as NF-κB and MAPK, Lim SM et al. [28]. In current study, we found that the ameliorative effect Sar sheds on chondrocytes in OA progression mainly rely on the activation of YAP1, which is a key node of Hippo pathway. In Lim's study, in addition to inhibiting the activation of NF-kB and MAPK pathways, the anti-inflammatory agent Sar impedes the binding of LPS to macrophage Toll-like receptor 4, and also regulates the polarization of M2 to M1 macrophages. These findings collectively suggest that in order to successfully manage OA, factors such as the

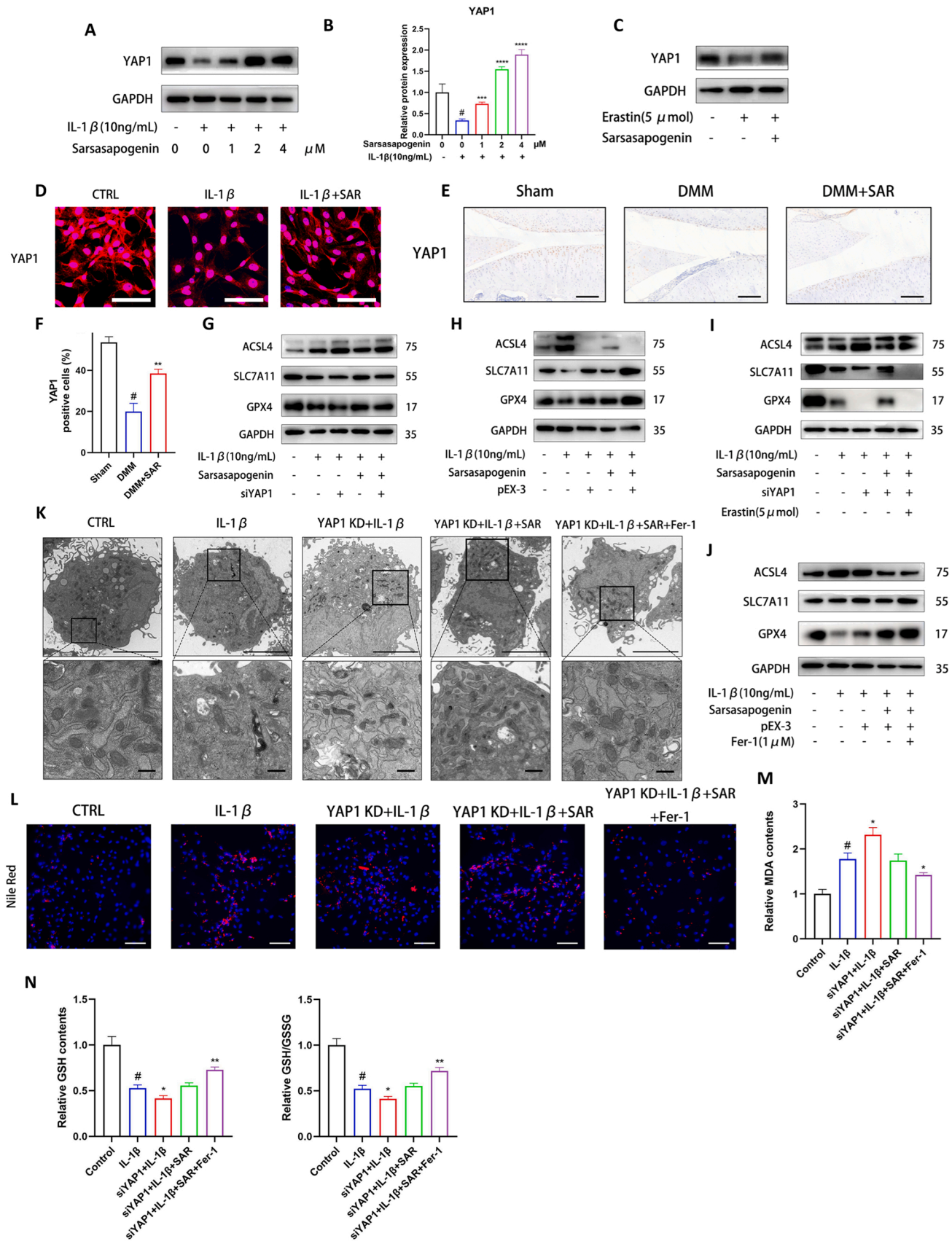

(caption on next page)

Fig. 5. By enhancing the expression of YAP1, Sar reduces the sensitivity of chondrocytes to ferroptosis. A-B) Western blot results and quantitative analysis of YAP1 of chondrocytes 24 h post indicated treatments, n = 3. C) Western blot results of YAP1 expression after the indicated treatment of erastin (5 μmol). D) Immunofluorescence for antibody against YAP1. Red, YAP1; Blue, DAPI; Scale bar = 100 μm E-F) Immunohistochemistry and quantitative analysis for antibody against Yap1. Scale bars = 200 μM. G-J) Western blotting analyses of the Gpx4, Slc7a11 and Acsl4 of chondrocytes 24 h post indicated treatments. Sar= 4 μM K) Transmission electron micrographs of chondrocytes samples post indicated treatments demonstrating morphological alterations in mitochondria. Scar bars, up, 5 μM; down, 400 nm. L) Representative images of chondrocytes 24 h post prescribed treatments stained with Nile Red to detect LDs. Scale bars = 100 μm. M) MDA measurement 24 h post prescribed treatment. n = 3. N) GSH contents and ratio of GSH/GSSG measurements. n = 3. All quantified data are shown as mean ± SD; #p < 0.05, *p < 0.05, **p < 0.01, ***p < 0.001, ****p < 0.0001 by one-way ANOVA followed by the Tukey- Kramer test.

pathogenic mechanism of OA, cell sensitivity, administration method, and length of treatment should be further taken into account.

An essential treatment strategy for treating OA has been thought to be focusing on chondrocyte death. According to findings from recent studies, ferroptosis plays a role in the progression of OA [24]. Previous studies revealed that a number of ferroptosis-related characteristics, including abnormal iron metabolism [25,26], lipid peroxidation [45, 46], and mitochondrial dysfunction [47,48], are strongly associated with hastening cartilage destruction. According to our research, Sar effectively inhibits ferroptosis of chondrocytes through promoting YAP1, which contributes to the preservation of osteoarthritic cartilage. Studies has proved that Sar has therapeutic potential on diseases like diabetic nephropathy through inhibiting cell autophagy by targeting GSK3β signaling pathway [49]. In fact, a growing body of research suggests that autophagy and ferroptosis are intrinsically linked. Some studies found that autophagy controls cellular iron homeostasis and ROS production, performing the role of an upstream mechanism in the process of ferroptosis induction [50,51]. Recent research also found that these two types of cell death were mediated by the YAP1 and GSK3 pathways, respectively. For instance, the research done by Huang and colleagues showed that a lack of liver TGFr1 prevented LPS/D-Gal-N-induced apoptosis and ferroptosis by having an effect on the phosphorylation of GSK3 [52]. Yet, the relationship between the autophagy and ferroptosis remains unknown, it is necessary to obtain additional experimental evidence in the future to determine if there are other mechanisms involved in regulating chondrocyte fate that contribute to the therapeutic effect of Sar in osteoarthritis.

It is widely recognized that the activity of YAP1, a key component of the Hippo signaling and a crucial regulator of OA, decreases during the development of OA [35,36]. Several mechanisms through which YAP1 regulates OA have been identified to date. On the one hand, by inhibiting NF-κB signaling, the role of YAP1 in regulating the Hippo pathway and its impact on maintaining articular cartilage homeostasis in OA is elucidated [35]. On the other hand, the collaboration between Yes-associated protein (YAP) and the transcriptional factor TEA domain (TEAD) contributes to the activation of the expression of the geroprotective protein known as forkhead box D1 (FOXD1), the rejuvenation of aged human mesenchymal stem cells (hMSCs) and the preservation of OA progression in mice were achieved through the overexpression of the YAP-FOXD1 axis [53]. Our initial findings have unveiled a novel mechanism by which YAP1 contributes to the progression of osteoarthritis that we have observed that YAP1 enhances cell death through the regulation of ferroptosis, accumulation of reactive oxygen species (ROS), and oxidation of lipids. The results of our study present a new discovery that YAP1 plays a role in the degeneration of osteoarthritic cartilage by converting chondrocytes into cells that are not susceptible to ferroptosis. This contributes to our knowledge of the therapeutic potential of YAP1 in managing osteoarthritis, and also offers fresh insights into the mechanisms that determine susceptibility to ferroptosis in the microenvironment of osteoarthritis.

It is undeniable that our research has some limitations. In contrast to apoptosis, the identification of ferroptosis lacks a universally accepted gold standard. However, we have substantiated the occurrence of ferroptosis in accordance with the definition provided by the Nomenclature Committee on Cell Death. Furthermore, it should be noted that due to the limited proliferative capacity of adult human chondrocytes, the progression of OA may require a significant amount of time, potentially taking several years or even decades, which means that chondrocyte damage and cell death will increase as OA progresses. In our study, we only gave chondrocytes a 48-hour treatment in vitro and cell proliferation can partially reverse chondrocyte ferroptosis. As a result, chondrocyte ferroptosis was underestimated in our study. Thirdly, gene knockdown and overexpression have not been used in animal experiments. Nonetheless, the outcomes are statistically significant, and the limitations have no bearing on the conclusion.

In summary, our research has shown a previously unidentified role for Sar in impeding OA progression by suppressing ferroptosis through the enhancement of YAP1, offering a novel therapeutic approach that is both solid and effective for the treatment of OA and other diseases associated with ferroptosis. (Fig. 6).

Funding

This study was funded by the Natural Science Foundation of Zhejiang Province (LD19H060004, LY21H060006) and Zhejiang Provincial Medical and Health Science and Technology Program (2023KY749).

CRediT authorship contribution statement

Weiping Chen designed this study, Study conduct: Ruihan Chen, Changjian Lin and Yuxuan Zou. Analysis and interpretation of data: Chenting Ying and Qiangchang Fu. Drafting the article: Ruihan Chen and Zhihui Xiang. Revising manuscript content and approving final version of manuscript: Jiapeng Bao and Weiping Chen. Jiapeng Bao helped revise the manuscript, helped edit the manuscript with the comments raised by reviewers. In the revision part, Jiapeng Bao made constructive suggestions on the comments about YAP1 pathway, checked and further confirmed the standardization of words and dictions.

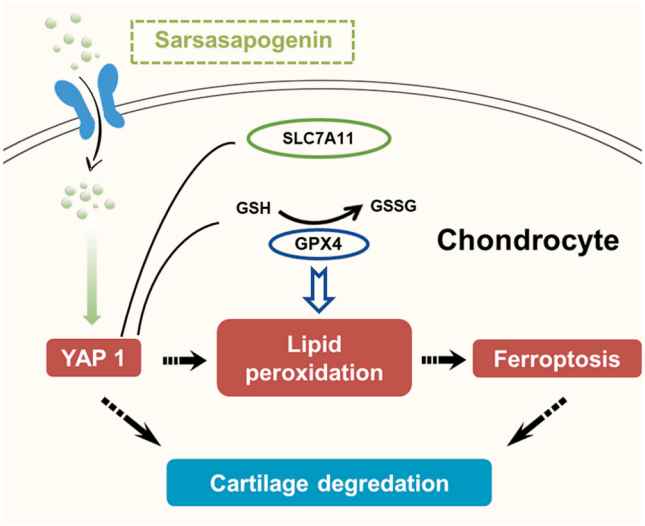

Fig. 6. In OA cartilage, Sar inhibits osteoarthritis progression by suppressing chondrocyte ferroptosis in a YAP1-dependent way. Sar prevented cartilage degradation by inhibiting chondrocyte ferroptosis via increasing YAP1 during OA progression.

Declaration of Competing Interest

The authors declare that they have no known competing financial interests or personal relationships that could have appeared to influence the work reported in this paper.

Data Availability

The study's original contributions are available in the article/Supplemental Material; any inquiries can be referred to the respective authors.

References

[1] S. Glyn-Jones, A.J. Palmer, R. Agricola, et al., Osteoarthritis, Lancet 386 (9991) (2015) 376–387.
[2] D.J. Hunter, S. Bierma-Zeinstra, Osteoarthritis, Lancet 393 (10182) (2019) 1745–1759.
[3] J.W. Michael, K.U. Schlüter-Brust, P. Eysel, The epidemiology, etiology, diagnosis, and treatment of osteoarthritis of the knee, Dtsch Arztebl Int. 107 (2010) 152–162.
[4] M. Chojnacki, A. Kwapisz, M. Synder, J. Szemraj, Osteoarthritis: etiology, risk factors, molecular mechanisms, Post. Hig. Med. Dosw. 68 (2014) 640–652.
[5] J.H. Kim, J. Jeon, M. Shin, et al., Regulation of the catabolic cascade in osteoarthritis by the zinc-ZIP8-MTF1 axis, Cell 156 (4) (2014) 730–743.
[6] D. Chen, J. Shen, W. Zhao, et al., Osteoarthritis: toward a comprehensive understanding of pathological mechanism, Bone Res. 5 (2017), 16044.
[7] C.B. Little, D.J. Hunter, Post-traumatic osteoarthritis: from mouse models to clinical trials, Nat. Rev. Rheumatol. 9 (8) (2013) 485–497.
[8] R.F. Loeser, S.R. Goldring, C.R. Scanzello, M.B. Goldring, Osteoarthritis: a disease of the joint as an organ, Arthritis Rheumatol. 64 (6) (2012) 1697–1707.
[9] M. Husa, R. Liu-Bryan, R. Terkeltaub, Shifting HIFs in osteoarthritis, Nat. Med. 16 (6) (2010) 641–644.
[10] A.C. Lin, B.L. Seeto, J.M. Bartoszko, et al., Modulating hedgehog signaling can attenuate the severity of osteoarthritis, Nat. Med. 15 (12) (2009) 1421–1425.
[11] C.B. Carballo, Y. Nakagawa, I. Sekiya, S.A. Rodeo, Basic science of articular cartilage, Clin. Sports Med. 36 (3) (2017) 413–425.
[12] E. Charlier, B. Relic, C. Deroyer, et al., Insights on molecular mechanisms of chondrocytes death in osteoarthritis, Int. J. Mol. Sci. 17 (12) (2016).
[13] L. Zheng, Z. Zhang, P. Sheng, A. Mobasheri, The role of metabolism in chondrocyte dysfunction and the progression of osteoarthritis, Ageing Res. Rev. 66 (2021), 101249.
[14] S. Jiang, Y. Liu, B. Xu, Y. Zhang, M. Yang, Noncoding RNAs: new regulatory code in chondrocyte apoptosis and autophagy, Wiley Inter. Rev. RNA (2020), e1584, 2020-01-10.
[15] S.J. Dixon, K.M. Lemberg, M.R. Lamprecht, et al., Ferroptosis: an iron- dependent form of nonapoptotic cell death, Cell 149 (2012) 1060–1072.
[16] B.R. Stockwell, J.P. Friedmann Angeli, H. Bayir, et al., Ferroptosis: a regulated cell death nexus linking metabolism, redox biology, and disease, Cell 171 (2017) 273–285.
[17] L. Galluzzi, I. Vitale, S.A. Aaronson, et al., Molecular mechanisms of cell death: recommendations of the Nomenclature Committee on Cell Death 2018, Cell Death Differ. 25 (2018) 486–541.
[18] T.M. Seibt, B. Proneth, M. Conrad, Role of Gpx4 in ferroptosis and its pharmacological implication, Free Radic. Biol. Med. 133 (2019) 144–152, 2019-03-01.
[19] W.S. Yang, R. SriRamaratnam, M.E. Welsch, et al., Regulation of ferroptotic cancer cell death by Gpx4, Cell 156 (1–2) (2014) 317–331.
[20] H. Lee, F. Zandkarimi, Y. Zhang, et al., Energy-stress-mediated AMPK activation inhibits ferroptosis, Nat. Cell Biol. 22 (2) (2020) 225–234.
[21] J. Lewerenz, S.J. Hewett, Y. Huang, M. Lambros, P.W. Gout, P.W. Kalivas, et al., The cystine/glutamate antiporter system x(c)(-) in health and disease: from molecular mechanisms to novel therapeutic opportunities, Antioxid. Redox Signal 18 (5) (2013) 522–555, 2013-02-10.
[22] X. Chen, J. Li, R. Kang, D.J. Klionsky, D. Tang, et al., Ferroptosis: machinery and regulation, Autophagy 17 (9) (2021) 2054–2081.
[23] B.R. Stockwell, A.J. Friedmann, H. Bayir, A.I. Bush, M. Conrad, S.J. Dixon, et al., Ferroptosis: a regulated cell death nexus linking metabolism, redox biology, and disease, Cell 171 (2) (2017) 273–285, 2017-10-05.
[24] Y. Miao, Y. Chen, F. Xue, et al., Contribution of ferroptosis and Gpx4's dual functions to osteoarthritis progression, EBioMedicine 76 (2022), 103847.
[25] X. Jing, J. Lin, T. Du, et al., Iron overload is associated with accelerated progression of osteoarthritis: the role of DMT1 mediated iron homeostasis, Front. Cell Dev. Biol. 8 (2020), 594509.
[26] M. Simao, P.J. Gavaia, A. Camacho, et al., Intracellular iron uptake is favored in Hfe- KO mouse primary chondrocytes mimicking an osteoarthritis- related phenotype, BioFactors 45 (2019) 583–597.
[27] Y.M. Zhang, T. Zheng, T.T. Huang, et al., Sarsasapogenin attenuates Alzheimer-like encephalopathy in diabetes, Phytomedicine 91 (2021), 153686.
[28] S.M. Lim, J.J. Jeong, G.D. Kang, et al., Timosaponin AIII and its metabolite sarsasapogenin ameliorate colitis in mice by inhibiting NF-κB and MAPK activation and restoring Th17/Treg cell balance, Int Immunopharmacol. 25 (2) (2015) 493–503.
[29] J. Saklatvala, Inflammatory signaling in cartilage: MAPK and NF-kappaB pathways in chondrocytes and the use of inhibitors for research into pathogenesis and therapy of osteoarthritis, Curr. Drug Targets 8 (2) (2007) 305–313.
[30] W. Bao, H. Pan, M. Lu, et al., The apoptotic effect of sarsasapogenin from Anemarrhena asphodeloides on HepG2 human hepatoma cells, Cell Biol. Int 31 (9) (2007) 887–892.
[31] D. Ma, J. Zhang, K. Sugahara, et al., Effect of sarsasapogenin and its derivatives on the stimulus coupled responses of human neutrophils, Clin. Chim. Acta 314 (1–2) (2001) 107–112.
[32] T. Sidiq, A. Khajuria, P. Suden, et al., A novel sarsasapogenin glycoside from Asparagus racemosus elicits protective immune responses against HBsAg, Immunol. Lett. 135 (1–2) (2011 30) 129–135.
[33] Pan, D. Hippo signaling in organ size control. Genes Dev. 21, 886–897, 2007.
[34] B. Zhao, K. Tumaneng, K.L. Guan, The Hippo pathway in organ size control, tissue regeneration and stem cell self-renewal, Nat. Cell Biol. 13 (2011) 877–883.
[35] Y. Deng, J. Lu, W. Li, et al., Reciprocal inhibition of YAP/TAZ and NF-κB regulates osteoarthritic cartilage degradation, Nat. Commun. 9 (1) (2018) 4564.
[36] Y. Gong, S.J. Li, R. Liu, et al., Inhibition of YAP with siRNA prevents cartilage degradation and ameliorates osteoarthritis development, J. Mol. Med. 97 (1) (2019) 103–114.
[37] J. Wu, A.M. Minikes, M. Gao, et al., Intercellular interaction dictates cancer cell ferroptosis via NF2-YAP signalling, Nature 572 (7769) (2019) 402–406.
[38] R. Gao, R. Kalathur, M. Coto-Llerena, et al., YAP/TAZ and ATF4 drive resistance to Sorafenib in hepatocellular carcinoma by preventing ferroptosis, EMBO Mol. Med. 13 (12) (2021), e14351.
[39] S.S. Glasson, M.G. Chambers, W.B. Van Den Berg, C.B. Little, The OARSI histopathology initiative - recommendations for histological assessments of osteoarthritis in the mouse, Osteoarthr. Cartil. 18 (Suppl 3) (2010) S17–S23.
[40] H. Miess, B. Dankworth, A.M. Gouw, et al., The glutathione redox system is essential to prevent ferroptosis caused by impaired lipid metabolism in clear cell renal cell carcinoma, Oncogene 37 (2018) 5435–5450.
[41] X. Chen, C. Yu, R. Kang, G. Kroemer, D. Tang, Cellular degradation systems in ferroptosis, Cell Death Differ. 28 (2021) 1135–1148.
[42] T. Petan, Lipid Droplets in Cancer. Rev Physiol Biochem Pharmacol., Springer, Berlin, Heidelberg, 2020, 1- 34.
[43] S. Dolma, S.L. Lessnick, W.C. Hahn, B.R. Stockwell, Identification of genotype-selective antitumor agents using synthetic lethal chemical screening in engineered human tumor cells, Cancer Cell 3 (2003) 285–296.
[44] L. Kong, Y. Liu, Y.M. Zhang, et al., Sarsasapogenin ameliorates diabetes-associated memory impairment and neuroinflammation through down-regulation of PAR-1 receptor, Phytother. Res 35 (6) (2021) 3167–3180.
[45] A. Ioan- Facsinay, M. Kloppenburg, Bioactive lipids in osteoarthritis: risk or benefit? Curr. Opin. Rheumatol. 30 (2018) 108–113.
[46] H. Jónasdóttir, H. Brouwers, J. Kwekkeboom, et al., Targeted lipidomics reveals activation of resolution pathways in knee osteoarthritis in humans, Osteoarthr. Cartil. 25 (2017) 1150–1160.
[47] R.S. Lane, Y. Fu, S. Matsuzaki, et al., Mitochondrial respiration and redox coupling in articular chondrocytes, Arthritis Res. Ther. 17 (2015), 54.
[48] C. Yang, D. You, J. Huang, et al., Effects of AURKA- mediated degradation of SOD2 on mitochondrial dysfunction and cartilage homeostasis in osteoarthritis, J. Cell Physiol. 234 (2019) 17727–17738.
[49] X.Z. Li, H. Jiang, L. Xu, et al., Sarsasapogenin restores podocyte autophagy in diabetic nephropathy by targeting GSK3β signaling pathway, Biochem Pharmacol. 192 (2021), 114675.
[50] D. Tang, X. Chen, R. Kang, G. Kroemer, Ferroptosis: molecular mechanisms and health implications, Cell Res. 31 (2) (2021) 107–125.
[51] M. Yang, P. Chen, J. Liu, et al., Clockophagy is a novel selective autophagy process favoring ferroptosis, Sci. Adv. 5 (2019), eaaw2238.
[52] S. Huang, Y. Wang, S. Xie, et al., Hepatic TGFβr1 deficiency attenuates lipopolysaccharide/D-galactosamine-induced acute liver failure through inhibiting GSK3β-Nrf2-mediated hepatocyte apoptosis and ferroptosis, Cell Mol. Gastroenterol. Hepatol. 13 (6) (2022) 1649–1672.
[53] L. Fu, Y. Hu, M. Song, et al., Up-regulation of FOXD1 by YAP alleviates senescence and osteoarthritis, PLoS Biol. 17 (4) (2019), e3000201.